International Journal of Recent Technology and Engineering (IJRTE)
ISSN: 2277-3878 (Online), Volume-8, Issue-1, May 2019

Concurrent Multi-Band Filters using Plasmonic High Resonance Step Impedance Resonator

P. Osman, P V Sridevi, K V S N Raju

Abstract*: This article reports the basic transmission line characteristics of metal-insulator-metal (MIM) wave guiding structure, design of band pass and band stop filter using a high resonance step impedance resonator (HRSIR). The effective refractive index, propagation length and characteristic impedance of the MIM wave guiding structure are obtained through full wave simulation. The proposed design of band pass and band stop filters operates simultaneously at optical frequency bands at 185.72 THz and 230.02 THz. The variation of designed plots are used to determine appropriate geometric parameters of each step when filter specification is given. Hence, the designed filters open a new way for the designing of integrated photonic devices based on surface plasmons.

***Index Terms*: MIM, Wave guiding structure, HRSIR, Sub-wavelength, Plasmonics.**

I. INTRODUCTION

Nano plasmonics offers an extensive awareness as a new technical innovation to overcome the diffraction limit for reducing the size of the photonic integrated circuits into nano-scale [1]. The limitations of the light wave in subwavelength scale lead through the localization and surface plasmons propagation along the interface of metal-insulator-metal (MIM) wave guiding structure. Metals are dealt with lossy plasma, which can be different from the idea of lossy conductor or ideal conductor principles used at GHz frequencies. The propagating surface wave along the metal-insulator interface using its supporting slow wave plasma obtaining lesser phase velocity, shortest wavelength, and larger wave impedance as compared to normal wave in the medium. The mode of the wave is identical to TEM mode; thus the supporting structures are designed by an equivalent transmission line.

Different nanoplasmonic wave guiding structure s have been proposed to achieve the photonic integrated circuits like insulator-metal-insulator (IMI) wave guiding structure , metal-insulator-metal (MIM) wave guiding structure [2] and nano-wires [3]. Because of its subwavelength nature and the maximum degree of light internment, MIM wave guiding structure has been identified perfectly suitable such systems [4]. Several surface Plasmon polaritons (SPPs) based MIM wave guiding structure devices have been demonstrated numerically and experimentally, such as tooth shaped filters [5], bends [6], bio sensors [7], Mach-Zehnder interferometers [8], Bragg reflectors [9], plasmonic switches [10], and multiplexers [11]. How each one of these circuit elements has been designed for single band frequency operation at a time.

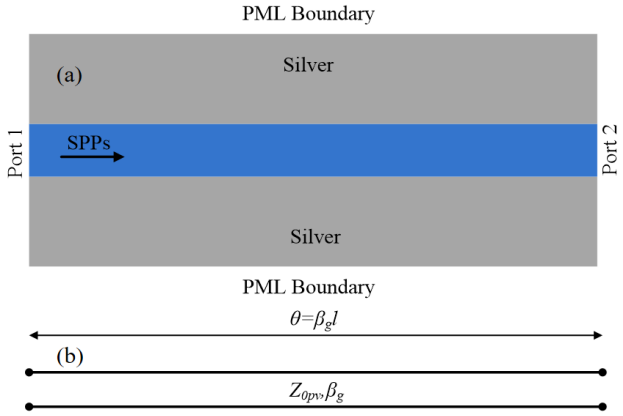

Fig.1 (a) Schematic of nanoplasmonic MIM guiding structure and (b)Two wire Transmission line equivalent circuit

Recently [12], [13], has reported the concurrent dual band band-pass filters in odd mode (RZ = Z2/Z1 < 1) case and a plasmonic dual band antenna for photonic integrated circuits (PICs). The main focus of this letter is to design the concurrent dual band band-pass filters using even mode condition (RZ = Z2/Z1 > 1) for PICs, due to the electric field in this condition is even mode. The proposed dual band filters have been designed using planar plasmonic MIM wave guiding structure. Transmission line characteristics of MIM wave guiding structure, dual band band-pass filter and band-stop filter characteristics of step impedance resonator (SIR) have been described. To obtain the numerical results of the design, full-wave analysis solver (CST Microwave studio suite) have been used.

Section II of this paper describes the MIM wave guiding structure and its equivalent characteristics of transmission line like effective refractive index (neff), surface plasmon polaritons propagation length (LSPP) and characteristic impedance (ZPV). In Section III and Section IV, characteristics of band-pass filter like transmission and insertion loss and band stop filter characteristics have been described. Finally, some conclusions about band-pass and band-stop filters in nano-scale MIM wave guiding structure s are summarized in section V.

Revised Manuscript Received on 30 May 2019.
***** Correspondence Author
P. Osman*, Department of Electronics and Communication Engineering, Samuel George Institute of Engineering & Technology, Markapur, Andhra Pradesh, India.
P V Sridevi, Department of Electronics and Communication Engineering, A U College of Engineering (A), Andhra University,Vishakapatnam, Andhra Pradesh, India.
K V S N Raju, Department of ECE, S.R.K.R.Engineering College, Bhimavaram, Andhra Pradesh, India.

II. BASIC CHARACTERISTICS OF PLASMONIC MIM WAVE GUIDING STRUCTURE

The plasmonic MIM wave guiding structure composed of two metal plates and dielectric material (ε_{SiO2} = 2.5) with the thickness (w), as shown in Fig. 1. The thickness of the dielectric material is used to ensure the deep subwavelength operation of the single mode operation. By indicating the characteristic impedance and effective refractive index (n_{eff}), plasmonic MIM wave guiding structure can be designed like a two-wire transmission line. The SPPs are created on two metal surfaces of the interface due to transverse magnetic (TM) plane-polarized incident light is coupled into the wave guiding structure. By applying the well-known Drude model, silver is assumed as a metal and its complex permittivity can characterize by [14]

$$\varepsilon(m) = 1 - \frac{\omega_p^2}{\omega(\omega + i\gamma_p^2)} \quad (1)$$

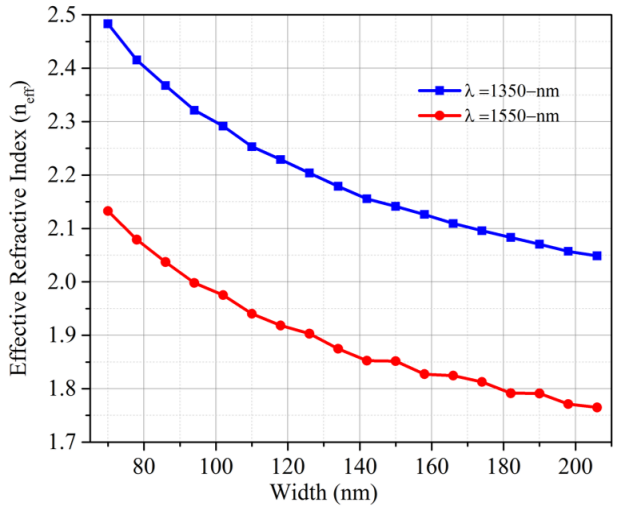

Fig.2 Effective refractive index with width (w) at Wavelengths (λ) 1350 nm and 1550 nm

Where $\omega_p = 1.38\times10^{16}$ rad/sec and $\gamma_p = 2.73\times10^{13}$ rad/sec Throughout the simulations, the outer boundaries of plasmonic MIM wave guiding structure excluding the input and output ports are selected for perfectly matched layer (PML) as shown in Fig. 1(a). Because, the wave propagates through the dielectric medium, the compatible definition of the characteristic impedance given by using the relation, $Z_{PV} = V^2/P$. Here the characteristic impedance depends on voltage and power i.e. $Z_{PV} = V^2/P$.

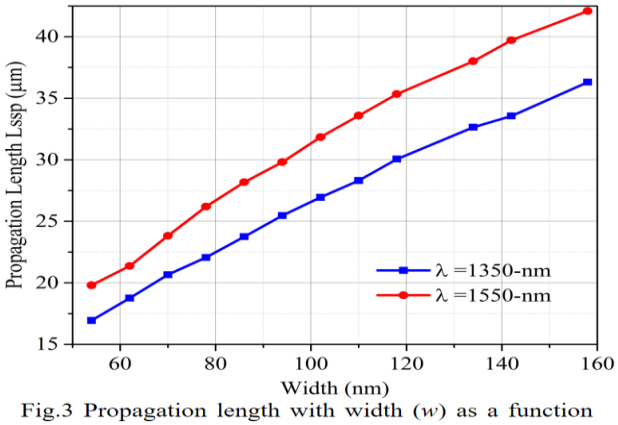

Fig.3 Propagation length with width (w) as a function of Wavelengths(λ) 1350 nm and 1550 nm

The line impedance is characterized around the ports that will combine the electric field and in the same way in order to determine the voltage, whereas power (P) will be calculate by the complex Poynting vector (E × H) across surface of the port. The real and imaginary part of the propagation constant can define by $\gamma = \alpha + j\beta$. The real part of the propagation constant (γ) is related to the propagation length ($L_{spp} = 1/2\alpha$) is defined as the length for which the field intensity decays to 1/e of its initial value.

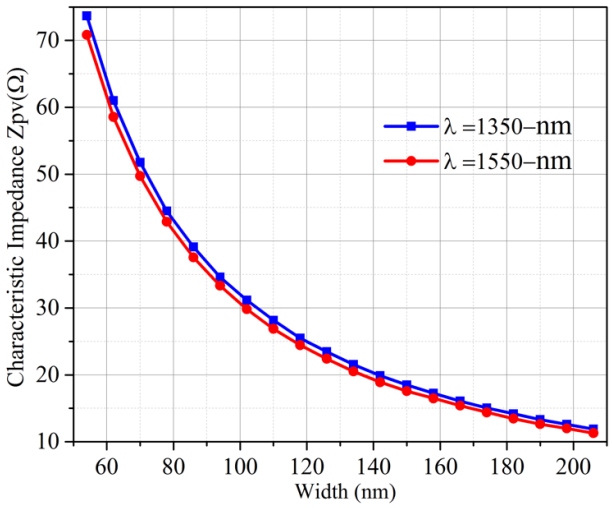

Fig.4 Characteristics impedance with width (w) as a function of Wavelengths(λ) 1350 nm and 1550 nm

Fig. 2 shows the variation of the effective refractive index (n_{eff}) with different wavelengths (1300 nm and 1600 nm) as a function of thickness (w) of the insulator. It's possible to give a conclusion from the figure that the effective refractive index (n_{eff}) increases with decreasing the dielectric gap-width (w). Fig. 3 shows the equivalent propagation length Lspp is calculated from the simulation data. Fig. 4 shows the similarity in characteristic impedance with different wavelengths (1300 nm and 1600 nm) as a function of gap width (w). By decreasing the slot width the characteristic impedance of the wave guiding structure increases. The higher impedance is around 85 dB for a gap width of 54 nm, whereas the lower feasible value is less than 15 dB.

III. CONCEPT OF HIGH RESONANCE STEP IMPEDANCE RESONATOR

The schematic of plasmonic MIM SIR with and their equivalent transmission line is shown in Fig. 5 with the comparison of [12]. The concept of even and odd mode λg/2 type MIM SIR have been proposed by Jankovic et.al [15]. Resonance occurs in each MIMSIR is either even or odd mode and the fundamental resonance occurs in the odd-mode case and in even-mode case first higher order resonance will occur and so forth. Thus, the resonance conditions are given by,

$$\tan\theta_1 = R_Z \cot\theta_2 \quad \text{(odd-mode)} \quad (2)$$

$$\tan\theta_2 = -R_Z \tan\theta_1 \quad \text{(even-mode)} \quad (3)$$

where R_Z is the ratio of impedances given by

$$R_Z = Z_2/Z_1 = \tan\theta_1 \tan\theta_2 \quad (4)$$

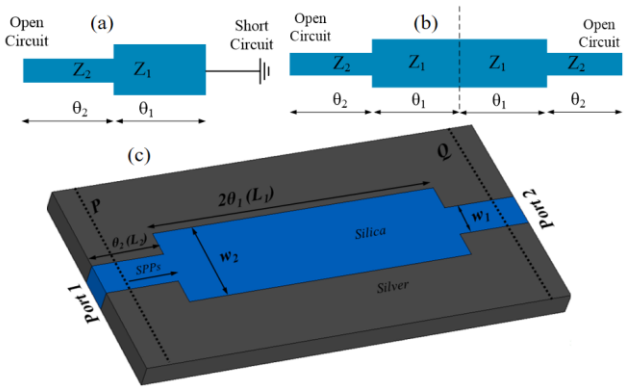

Fig.5 Geometries of Step Impedance Resonators (a) Quarter Wavelength (b) Half Wavelength (c) Plasmonic MIMSIR guiding Structure

As a result, resonance condition is dependent on the resonators electrical length and also the characteristic impedance ratio (R_Z). The equivalent circuits of both even and odd mode MIM SIR are sufficient to support the analysis of near resonance frequencies, then it is easy to understand the behavior of the circuit at resonance condition. The fundamental and spurious resonance frequency relationship for a special case of $\theta_1 = \theta_3 = \theta_0$ presented in [16], given by;

$$\lambda \frac{f_{S1}}{f_0} = \frac{\pi}{2\tan^{-1}\sqrt{R_Z}} \quad (5)$$

$$\lambda \frac{f_{S3}}{f_0} = \frac{\pi}{\tan^{-1}\sqrt{R_Z}} \quad (6)$$

Where f_0, $f_{S1}$and f_{S3} are centre, first and second spurious frequencies respectively.

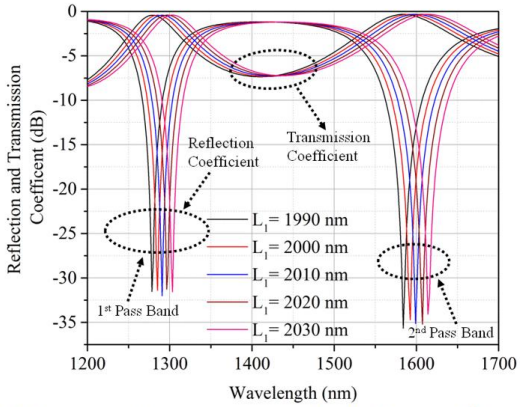

Fig.6 Variation of transmission and reflection coefficient with wavelength as a function of Length (L_1), L_2=1010 nm, w_1=420 nm, w_2=120 nm

By the concept of higher resonance mode SIR as discussed above, band-pass filter characteristics of MIM SIR have been determined by using CST Microwave Studio Suite based upon MIM wave guiding structure shown in Fig. 5. Input and output powers have been calculated by placing the power monitors P and Q at a distance of 1522.5 nm from the center of the plasmonic MIM SIR. In the full-wave simulations, the grid sizes are set to 5 nm × 5 nm along x and y directions. The fundamental TM mode of the plasmonic MIM wave guiding structure have been started from left to the right side of the wave guiding structure . The fundamental TM mode of wave guiding structure only can propagate, due to the width of the plasmonic wave guiding structure is smaller than the wavelength.

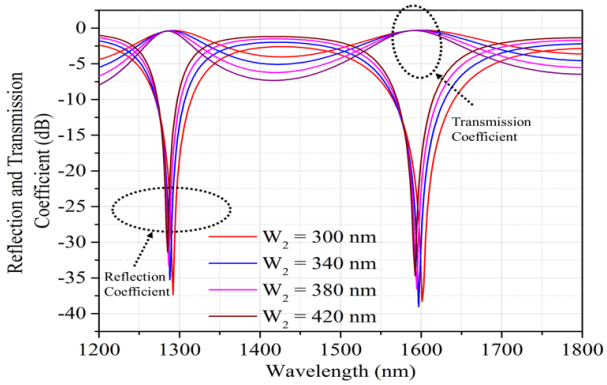

Fig.7 Variation of reflection and transmission coefficient with wavelength as a function of width(w_2) ,w_1=420 nm, lengths L_1=2020 nm, L_2=1010 nm

TABLE I
UNITS FOR MAGNETIC PROPERTIES

W_2 (nm)	λ_{01} (nm)	λ (nm)	$Q = \lambda_{01}/\lambda$	λ_{02} (nm)	λ (nm)	$Q = \lambda_{01}/\lambda$
180	1289	147	9	1596	267	6
200	1295	122	11	1604	218	7
220	1297	107	12	1605	187	9
240	1301	95	14	1610	166	10
260	1304	91	14	1613	150	11

Transmission coefficients of the filter are shown in Figs. 6 and 7. Since the object of our design is looking for a band-pass filter with the physical dimensions w_1 = 420 nm, w_2 = 120 nm, L_1 = 2020 nm, L_2 = 1010 nm. Using Eq. (5), resonance occurs at R_Z = 5.8712 and the first peak of the pass band appear at fundamental frequency f_0 = 185.72 THz (1614 nm) simultaneously the second peak of pass band appears at first spurious frequency f_{S1} = 230.02 THz (1303 nm) if $\theta_1 = \theta_2 = \theta_0$. However, the second peak of the pass band occurs at 1272 nm in place of 1303 nm as shown in Fig. 6. This kind of shift is possible, due to different electrical lengths θ_1 and θ_2, when the total electrical length of the resonator ($\theta_T = (\theta_1+\theta_2)$) is fixed. Fig. 6 and Fig. 7 shows the variation in transmission coefficients of the resonator with the parametric changes as a function of L_1 and w_2. It is clearly shown that the variation in length L_1 offers better impact when it is compared to width w_2. Table 1 shows the quality factor (Q) of the SIR of two pass bands with corresponding to the Fig. 6.

IV. MULTI BAND BAND-STOP FILTER

The schematic of the concurrent dual band band-stop filter (BSF) shown in Fig. 8. The dual band BSF is designed and simulated with the fixed dimensions at w_1 = 62 nm, w_2 = 100 nm, w_3 = 30 nm, w_3+2(L_1) = 2250 nm, lengths L_1 = 1050 nm, L_2 = 525 nm, L_3 = 500 nm. Fig. 9 shows the simultaneous transmission coefficients of the filter at wavelengths 1317 nm and 1606 nm as a function of w_2 when the widths w_1 and w_3 are fixed. Fig. 10 shows the magnitude of electric filed distribution at wavelengths 1606 nm and 1317 nm.

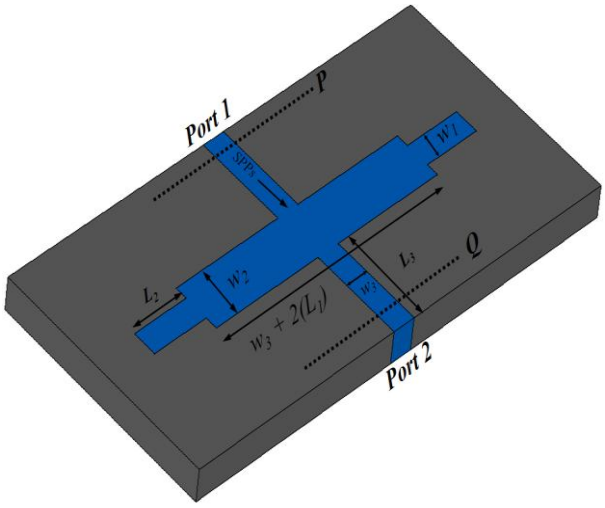

Fig.8 Geometry of the dual band MIMSIR based plasmonic Band Stop Filter for fixed widths w_1=62nm, w_2=100nm, w_3=30nm, w_3+2L_1=2250nm, lengths L_1=1050nm, L_2=525 nm, L_3=500nm

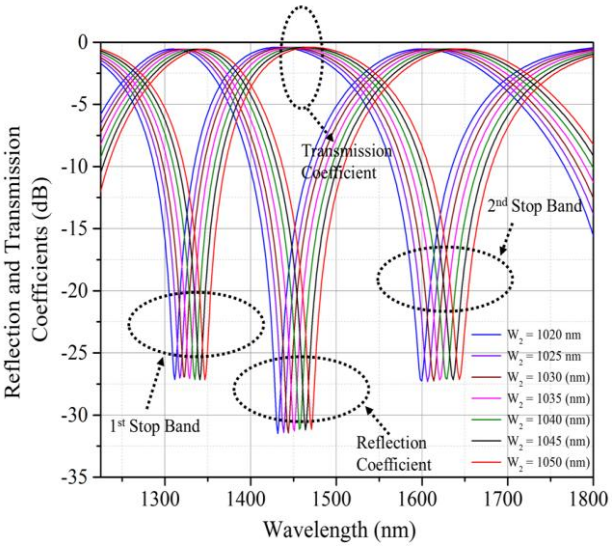

Fig.9 Variation of reflection and transmission coefficient with wavelength as a function of width(w_2) , w_1=62nm, w_3=30nm, w_3+2L_1=2250nm, lengths L_1=1050nm, L_2=525 nm, L_3=500nm

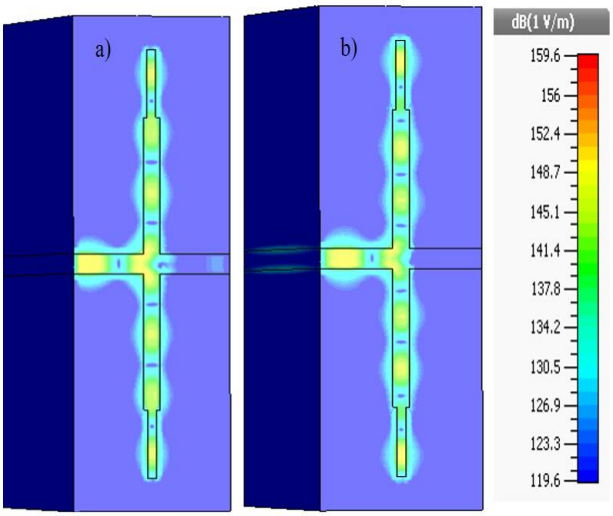

Fig.10 Field distribution at wavelength a)1606-nm b)1317-nm

V. CONCLUSION

The basic transmission line characteristics of MIM wave guiding structure have been studied and numerically analyzed. Using high resonance plasmonic step impedance resonator (HRSIR) a concurrent dual band band-pass and band-stop filter have designed and simulated. The basic characteristics of MIM wave guiding structure such as effective refractive index, propagation length and characteristic impedance are obtained through full wave simulations. The designed dual band band-pass and stop filters operates simultaneously at optical frequency bands at 185.72 THz and 230.02 THz. Hence, the designed filters open a new way for the designing of photonic integrated circuits based on surface plasmons.

REFERENCES

1. R. Zia, M. D. Selker, P. B. Catrysse, and M. L. Brongersma, “Geometries and materials for subwavelength surface plasmon modes,” J. Opt. Soc. Am. A, vol. 21, no. 12, pp. 2442-2446, July 2004.
2. Z. Han, “Ultracompact plasmonic racetrack resonators in metal-insulator-metal waveguides,” Photonics Nanostructures - Fundam. Appl., vol. 8, no. 3, pp. 172-176, Apr. 2010.
3. S. Mokkapati, D. Saxena, N. Jiang, H. H. Tan, and C. Jagadish, “Plasmonic cavities for increasing the radiative efficiency of GaAs nano wires,” 2014 Conf. Optoelectron. Microelectron. Mater. Devices, COMMAD 2014, vol. 1, pp. 244-245, Dec. 2014.
4. J. Qi et al., “Independently tunable double Fano resonances in asymmetric MIM waveguide structure,” Opt. Express, vol. 22, no. 12, pp. 14688-14695, Jun. 2014.
5. Xian-Shi Lin and Xu-Guang Huang, “Tooth-shaped plasmonic waveguide filters with nanometeric sizes 1,” Opt. Lett., vol. 33, no. 23, pp. 2874-2876, Dec. 2008.
6. A. M. Heikal, M. F. O. Hameed, and S. S. A. Obayya, “Coupling characteristic of a novel hybrid long-range plasmonic waveguide including bends,” IEEE J. Quantum Electron., vol. 49, no. 8, pp. 621-627, Aug. 2013.
7. L. Wu, P. Bai, X. Zhou, and E. P. Li, “Reflection and transmission modes in nanohole-array-based plasmonic sensors,” IEEE Photonics J., vol. 4, no. 1, pp. 26-33, Feb. 2012.
8. J. Gosciniak, L. Markey, A. Dereux, and S. I. Bozhevolnyi, “Thermo-optic control of dielectric-loaded plasmonic Mach-Zehnder interferometers and directional coupler switches,” Nanotechnology, vol. 23, no. 44, pp. 444008 (1-9), Oct. 2012.
9. S. Zhu, H. S. Chu, G. Q. Lo, and D. L. Kwong, “CMOS-compatible plasmonic bragg reflectors based on cu-dielectric-si structures,” IEEE Phot. Tech. Lett., vol. 25, no. 21, pp. 2115-2118, Nov. 2013.
10. Y. B. Zheng, et. al, “Incident-angle-modulated molecular plasmonic switches: A case of weak exciton-plasmon coupling,” Nano Lett., vol. 11, no. 5, pp. 2061-2065, Apr. 2011.
11. V. Liu, Y. Jiao, D. A. B. Miller, and S. Fan, “Design methodology for compact photonic-crystal-based wavelength division multiplexers,” Opt. Lett., vol. 36, no. 4, pp. 591-593, Feb. 2011.
12. Ravi Kiran Chityala, “Nanoplasmonic concurrent dual band antennas using metal-insulator-metal step impedance resonators,” Microwave and Optical Tech. Lett., Feb.2019.
13. K. Thirupathaiah, B. Iyer, N. Prasad Pathak, and V. Rastogi, “Concurrent dualband diplexer for nanoscale wireless links,” IEEE Photonics Technol. Lett., vol. 26, no. 18, pp. 1832-1835, Sep. 2014.
14. K. R. Hiremath, L. Zschiedrich, and F. Schmidt, “Numerical solution of nonlocal hydrodynamic Drude model for arbitrary shaped nano-plasmonic structures using Nédélec finite elements,” J. Comput. Phys., vol. 231, no. 17, pp. 5890-5896, May 2012.

15. N. Jankovic and V. Crnojevic, P. Meyer and J. Hong, “Design methods of multi-band filters,” EuMA High Freq. Tech. Seri., pp. 5-66, Jul. 2015.
16. M. Makimoto S. Yamashita, “Microwave Resonators and Filters for Wireless Communication,” Springer-Verlag Berlin Heidelberg,4th Edition.